

## Electronic Supplementary Information

# Facile Fabrication of Novel Highly Microporous Carbons with Superior Size-Selective Adsorption and Supercapacitance Properties

Zhenghui Li, Dingcai Wu,\* Yeru Liang, Fei Xu, Ruowen Fu

Materials Science Institute, PCFM Lab and DSAPM Lab, School of Chemistry and Chemical Engineering, Sun Yat-sen University, Guangzhou 510275, P. R. China

## Experimental

### Sample preparation

In a typical process, 12.0 g of anhydrous aluminium chloride ( $\text{AlCl}_3$ ) was added into 100 ml of carbon tetrachloride ( $\text{CCl}_4$ ) in a three-neck flask. Then the mixture was refluxed with magnetic stir for 40 min at 75 °C. Subsequently, a solution of 5.0 g of linear polystyrene resin dissolved in 100 ml of  $\text{CCl}_4$  was added to undergo a Friedel-Crafts crosslinking reaction. After 30 min, 100 ml of ethanol-water solution (95 wt. % ethanol/water = 80 ml/20 ml) was added slowly to stop the reaction. The product was filtered off, washed with the 95 wt.% ethanol/5 wt.% dilute hydrochloric acid mixture (150 ml/50 ml) and pure water, followed by drying at 100 °C for 8 h. After that, the as-obtained  $x\text{PS}$  was carbonized at 900 °C for 3 h in  $\text{N}_2$  flow with a heating rate of 2 °C/min, leading to formation of HMC. To investigate the nanostructure evolution,  $x\text{PS}$  was also treated at 320 and 460 °C to obtain  $x\text{PS-320}$  and  $x\text{PS-460}$ , respectively. For fabrication of  $u\text{HMC}$ , the procedure is exactly the same as that of HMC except that the used disposable polystyrene foam tableware, which was washed prior to utilization, was employed as the raw material.

---

\* Corresponding author. E-mail: [wude@mail.sysu.edu.cn](mailto:wude@mail.sysu.edu.cn)

## Structural Characterization

The thermogravimetric analysis (TGA) was performed with a heating rate of 5 °C/min in N<sub>2</sub> flow. Fourier transform infrared (FTIR) spectra were measured using a Bruker Equinox 55 FTIR spectroscopy. The morphologies of the samples were observed by a JSM-6330F scanning electron microscope (SEM) and a JEM-2010HR transmission electron microscope (TEM). The Raman spectrum was obtained with a Renishaw inVia Raman spectrometer. A Micromeritics ASAP 2010 surface area and porosity analyzer was used to investigate the pore structure. The BET surface area ( $S_{BET}$ ) was analyzed by Brunauer-Emmett-Teller (BET) theory. The micropore surface area ( $S_{mic}$ ) was determined by t-plot method. The total pore volume ( $V_t$ ) was calculated from the amount adsorbed at a relative pressure  $P/P_0$  of 0.997. The pore size distribution was analyzed by original density functional theory (DFT) with non-negative regularization and medium smoothing.

## Adsorption Characterization

Adsorption amounts of captopril and VB12 on carbon materials were obtained by measuring their concentrations before and after adsorption. 45 mg of carbon powder was added into a conical flask, and then 75 mL of captopril or VB12 solution (200 mg L<sup>-1</sup>) was added quickly. After that, this suspension was shaken with a rate of 150 rpm at 30 °C. At intervals, 0.5 mL of supernate was taken out and diluted to 5 mL. The concentration of adsorbate was measured by UV-Vis spectra. The wavelength for captopril and VB12 is 220 and 360 nm, respectively. The adsorption capacity (C) was calculated according to the equation  $C=(c_0V_0-c_1V_1)/(mS_{BET})$ , where  $c_0$ ,  $V_0$ ,  $c_1$ ,  $V_1$  and  $m$  represent the initial concentration, initial volume, concentration and volume after adsorption, and weight of carbon materials, respectively. The selectivity (S) is obtained according to the equation  $S=C_{cap}/C_{VB12}$ , where  $C_{cap}$  and  $C_{VB12}$  are the molar saturation adsorption capacity at 24 h for captopril and VB12, respectively.

## Electrochemical Characterization

The electrochemical performances of HMC were measured in 6 M KOH using a sandwich-type two-electrode testing cell at ambient condition. HMC electrodes in the form of round sheet were obtained by pressing a mixture film of 92 wt% HMC and 8 wt% polytetrafluorethylene into a nickel foam current collector. The mass of HMC in each electrode is about 10 mg. Galvanostatic charge–discharge test was executed at a current density of  $10 \text{ mA g}^{-1}$  over a voltage range of 0–1.0 V using Arbin BT2000 instrument. Cyclic voltammetry (CV) measurement was performed at a sweep rate of  $2 \text{ mV s}^{-1}$  with an IM6e electrochemical workstation from -1V to 0V. The specific capacitance ( $C_m$ ) was calculated according to the equation  $C_m = 2 \times I_m t / \Delta V$ , where  $I_m$ ,  $t$  and  $\Delta V$  represent the current density, the discharge time and the discharge voltage, respectively. The capacitance per surface area ( $C_s$ ) was calculated according to the equation  $C_s = C_m / S_{BET}$ , where  $S_{BET}$  is the BET surface area.

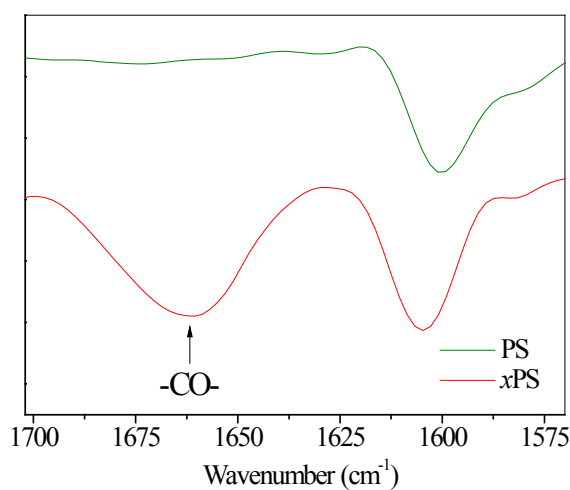
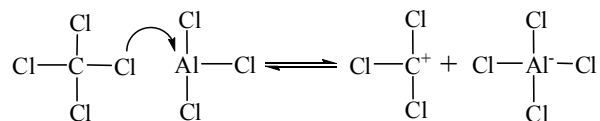
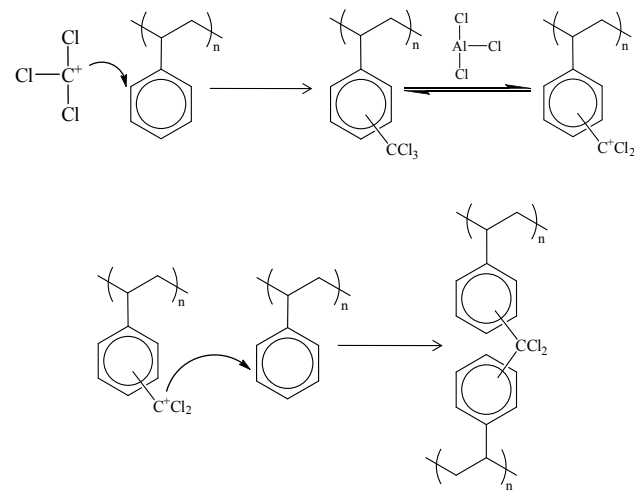


**Fig. S1** FT-IR spectrums of PS and xPS.

**(1) Formation of carbocation  $^{+}\text{CCl}_3$**



**(2) Formation of -CCl<sub>2</sub>- crosslinking bridges**



**(3) Formation of -CO- crosslinking bridges**

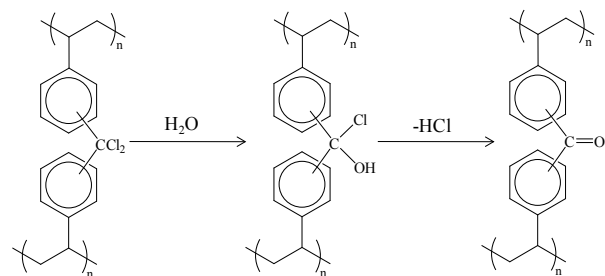


**Fig. S2** Formation mechanism of -CO- crosslinking bridge.<sup>1</sup>

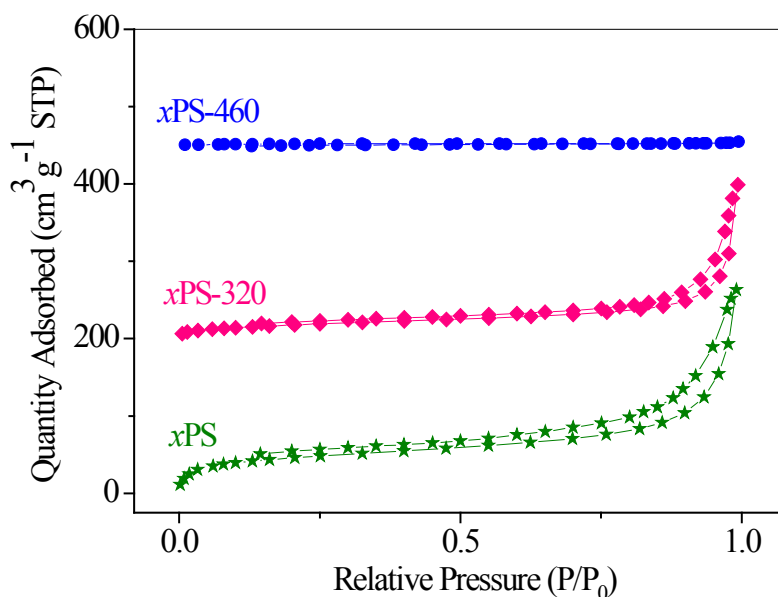


**Fig. S3** N<sub>2</sub> adsorption-desorption isotherms of xPSs.

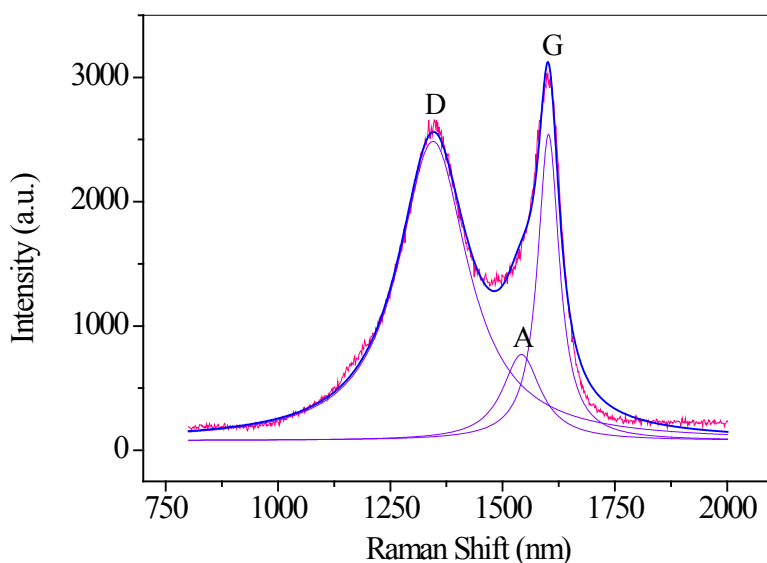


**Fig. S4** Raman spectrum of HMC. In the Raman spectrum, the band around 1602 cm<sup>-1</sup>, 1542 cm<sup>-1</sup>, and 1345 cm<sup>-1</sup> can be denoted as G (graphitic) peak, A (amorphous) peak and D (disordered) peak, respectively.<sup>2</sup> The microcrystalline planar crystal size  $L_a$  can be calculated using the empirical formula found by Tuinstra and Koeing ( $L_a = 4.35 I_G/I_D$  (nm)), where  $I_G$  and  $I_D$  are integrated intensity of G and D peak, respectively). For HMC,  $L_a$  is equal to 1.39 nm, indicating that HMC reveals a graphite-like microcrystalline structure.

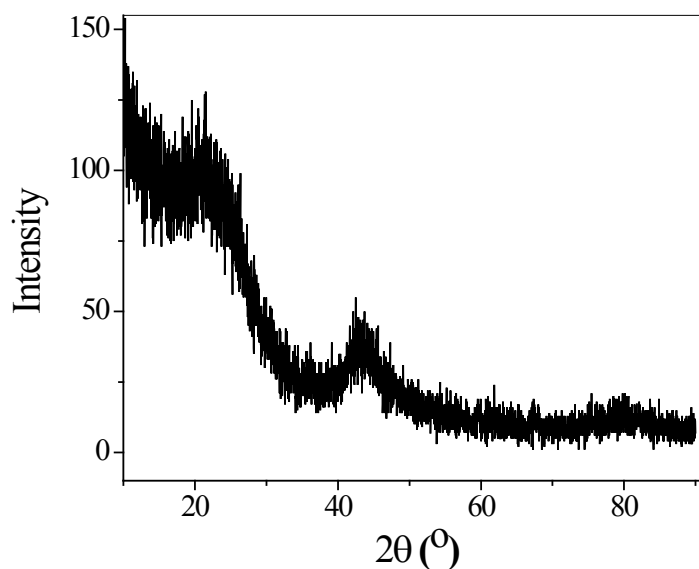


**Fig. S5** XRD pattern of HMC. HMC displays a broad and weak (002) diffraction peak at 22°, indicative of a graphite-like microcrystalline structure.

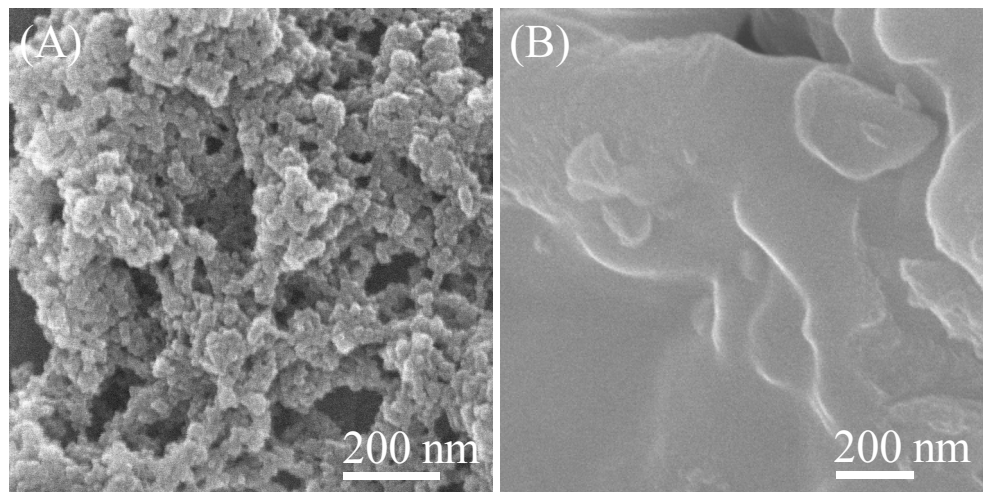


**Fig. S6** SEM images of (a) the lowly crosslinked PS (*u*xPS) and (B) its related carbon product (*u*HMC) prepared using the used disposable polystyrene foam tableware as the raw material.

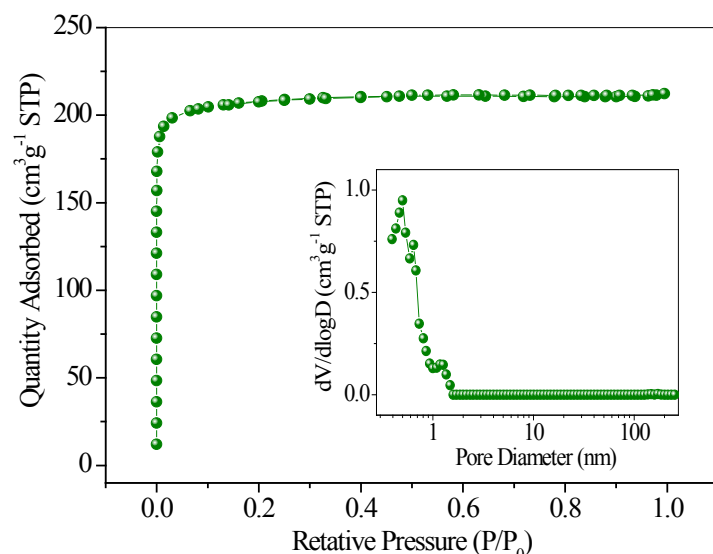


**Fig. S7** N<sub>2</sub> adsorption-desorption isotherm and DFT pore size distribution (inset) for uHMC.

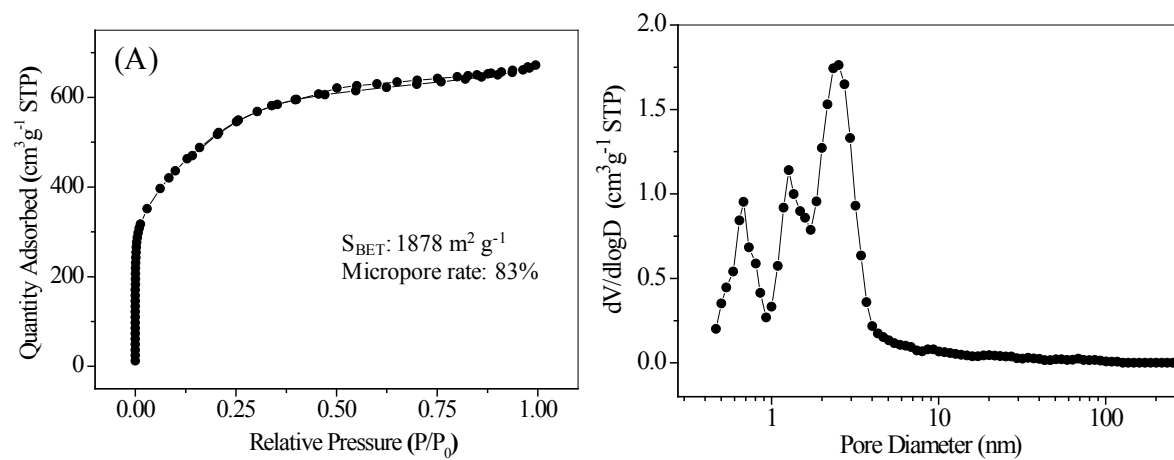


**Fig. S8** (A) N<sub>2</sub> adsorption-desorption isotherm and (B) DFT pore size distribution for AC.

**Table S1** Micropore rates of some typical microporous carbons.\*

No.	Sample	$S_{\text{BET}}$ ( $\text{m}^2 \text{g}^{-1}$ )	Micropore rate (%)		Reference
			Surface area	Volume	
1	<b>HMC</b>	<b>1108</b>	<b>97</b>	<b>93</b>	<b>This study</b>
2	PP carbon	1320-2260	-	46~59	3
3	PAN carbon	580	-	74	3
4	PFA carbon	590	-	65	3
5	N-C-1	1363	48	35	4
6	N-C-4	1329	49	42	4
7	CF900-4	1616	-	74	5
8	CFB900-4	1722	-	68	5
9	<b>AC</b>	<b>1878</b>	<b>83</b>	<b>71</b>	<b>This study</b>
10	Acticarbone 3S	1013	-	54	6
11	Norit SX 1G	1047	-	59	6
12	Norit SX2 POCH	835	79	-	7
13	AC	1585	-	41	8
14	AC-C4	1308	-	47	8
15	AC-K5	3190	-	64	8
16	AC-P600	2095	74	65	9
17	AC-P650	3246	47	39	9
18	AC-P700	3432	42	34	9
19	C34	1083	-	42	10
20	C46	1600	-	42	10
21	ACM-A	2652	69	72	11
22	ACM-C	403	78	85	11

23	DUT-38-A-850-6	2635	-	76	12
24	DUT-38-A-950-4	3104	-	60	12
25	K9-3/15	1576	-	83	13
26	K7-3/15	2438	-	70	13
27	K7-5/30	2875	-	54	13
28	popcarbon-600	589	86	-	14
29	popcarbon-750	773	84	-	14
30	popcarbon-900	1417	70	-	14
31	CS	430	-	87	15

\* Samples 2~8 are microporous templated carbons, sample 9-27 are activated carbons, and samples 28~31 are other microporous carbons.

**Table S2** Parameters of Raman spectrum of HMC.

Sample	Peak center ( $\text{cm}^{-1}$ )			% Peak area*			$L_a$ (nm)
	D	A	G	D	A	G	
HMC	1345	1542	1602	67.7	10.7	21.6	1.39

\* Peak area = area of peak X/(total area of peaks D, A and G), where X=D, A, G.

**Table S3** Structural formula of captopril and VB12.

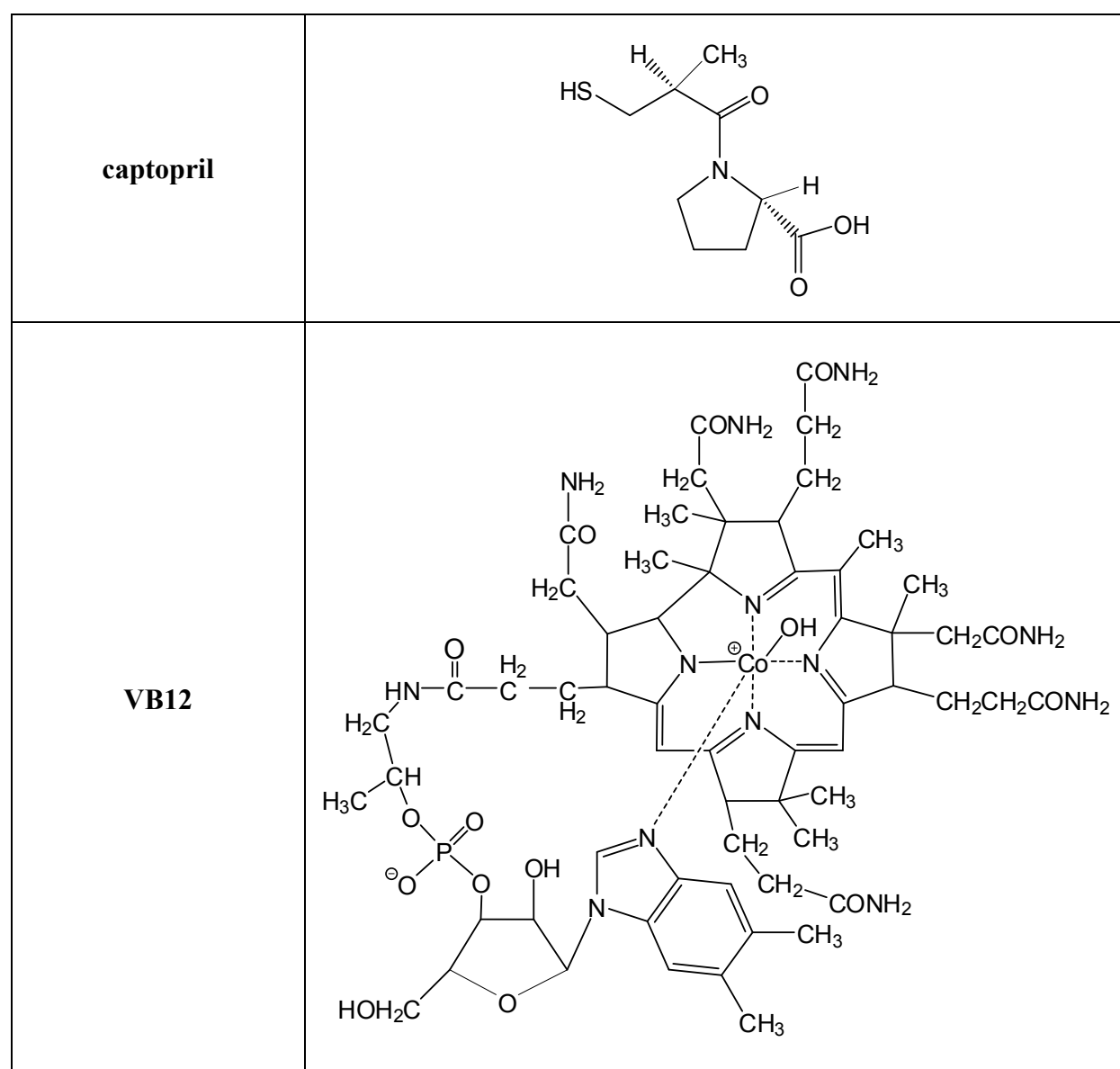


**Table S4** The capacitance per surface area ( $C_s$ ) of some typical microporous carbons.

No.	Sample	Measurement condition	Electrolyte	$C_s$ ( $\mu\text{F cm}^{-2}$ )	Reference
1	HMC	<b>10 mA g<sup>-1</sup></b>	<b>6M KOH</b>	<b>15.0</b>	<b>This study</b>
2	XC-72	5 mV s <sup>-1</sup>	2M H <sub>2</sub> SO <sub>4</sub>	8.8	16
3	Maxsorb	5~50 mV s <sup>-1</sup>	30% KOH	10.1~2.2	17
4	M30	1 mHz	30% KOH	2.4	18
5	SACF-20	1 mHz	30% KOH	2.7	18
6	A10	1 mHz	30% KOH	3.1	18
7	M10	1 mHz	30% KOH	4.1	18
8	TiC CDC	5 mV s <sup>-1</sup>	1M H <sub>2</sub> SO <sub>4</sub>	4.8~12.2	19
9	ZrC CDC	5 mV s <sup>-1</sup>	1M H <sub>2</sub> SO <sub>4</sub>	6.3~11.8	19
10	P-KOH-AC	10 mV s <sup>-1</sup>	1M NaNO <sub>3</sub>	9.3	20
11	CF	0.5~5 mA	1M H <sub>2</sub> SO <sub>4</sub>	9.4~8.8	21
12	CF01	0.5~5 mA	1M H <sub>2</sub> SO <sub>4</sub>	10~9.5	21
13	W-KOH-AC	10 mV s <sup>-1</sup>	1M NaNO <sub>3</sub>	10.9	20
14	LA/1	-	6M KOH	11.6	22
15	SA/S/1	-	6M KOH	11.9	22
16	CF03	0.5~5 mA	1M H <sub>2</sub> SO <sub>4</sub>	12.9~12.4	21
17	KJA	-	6M KOH	13.7	22
18	DCG-5	5 mV s <sup>-1</sup>	2M H <sub>2</sub> SO <sub>4</sub>	16.5	16
19	CMS	5 mV s <sup>-1</sup>	2M H <sub>2</sub> SO <sub>4</sub>	17.3	16

## References

1. D. C. Wu, A. Nese, J. Pietrasik, Y. R. Liang, H. K. He, M. Kruk, L. Huang, T. Kowalewski and K. Matyjaszewski, *Ac Nano*, 2012, **6**, 6208-6214.

2. D. C. Wu, H. C. Dong, J. Pietrasik, E. K. Kim, C. M. Hui, M. J. Zhong, M. Jaroniec, T. Kowalewski and K. Matyjaszewski, *Chem. Mater.*, 2011, **23**, 2024-2026.
3. T. Kyotani, T. Nagai, S. Inoue and A. Tomita, *Chem. Mater.*, 1997, **9**, 609-615.
4. G. P. Meisner and Q. Hu, *Nanotechnology*, 2009, **20**, 204023.
5. F. Su, J. Zeng, Y. Yu, L. Lv, J. Y. Lee and X. S. Zhao, *Carbon*, 2005, **43**, 2366-2373.
6. J. I. Paredes, A. Martinez-Alonso, P. X. Hou, T. Kyotani and J. M. D. Tascon, *Carbon*, 2006, **44**, 2469-2478.
7. G. Lota, T. A. Centeno, E. Frackowiak and F. Stoeckli, *Electrochim. Acta*, 2008, **53**, 2210-2216.
8. H. L. Wang, Q. M. Gao and J. Hu, *J. Am. Chem. Soc.*, 2009, **131**, 7016-7022.
9. L. Wei, M. Sevilla, A. B. Fuertes, R. Mokaya and G. Yushin, *Adv. Funct. Mater.*, 2012, **22**, 827-834.
10. C. H. Lei, N. Amini, F. Markoulidis, P. Wilson, S. Tennison and C. Lekakou, *J. Mater. Chem. A*, 2013, **1**, 6037-6042.
11. V. Ruiz, C. Blanco, R. Santamaria, J. M. Ramos-Fernandez, M. Martinez-Escandell, A. Sepulveda-Escribano and F. Rodriguez-Reinoso, *Carbon*, 2009, **47**, 195-200.
12. M. Oschatz, L. Borchardt, I. Senkovska, N. Klein, M. Leistner and S. Kaskel, *Carbon*, 2013, **56**, 139-145.
13. K. Babel, D. Janasiak and K. Jurewicz, *Carbon*, 2012, **50**, 5017-5026.
14. L. F. Wang, J. Zhang, D. S. Su, Y. Y. Ji, X. J. Cao and F. S. Xiao, *Chem. Mater.*, 2007, **19**, 2894-2897.
15. J. Choma, D. Jamiola, K. Augustynek, M. Marszewski, M. Gao and M. Jaroniec, *J. Mater. Chem.*, 2012, **22**, 12636-12642.
16. T. A. Centeno, M. Hahn, J. A. Fernández, R. Kötz, F. Stoeckli, *Electrochim. Commun.*, 2007, **9**, 1242-1246.

17. W. Xing, S. Z. Qiao, R. G. Ding, F. Li, G. Q. Lu, Z. F. Yan, H. M. Cheng, *Carbon*, 2006, **44**, 216-224.
18. D. Y. Qu, H. Shi, *J. Power Sources*, 1998, **74**, 99-107.
19. J. Chmiola, G. Yushin, R. Dash, Y. Gogotsi, *J. Power Sources*, 2006, **158**, 765–772.
20. F. C. Wu, R. L. Tseng, C. C. Hu, C. C. Wang, *J. Power Sources*, 2005, **144**, 302–309.
21. C. T. Hsieh, H. Teng, *Carbon*, 2002, **40**, 667-674.
22. G. Gryglewicz, J. Machnikowski, E. Lorenc-Grabowsk, G. Lota, E. Frackowiak, *Electrochim. Acta*, 2005, **50**, 1197-1206.